



ELSEVIER

Contents lists available at ScienceDirect

Journal of Petroleum Science and Engineering

journal homepage: www.elsevier.com/locate/petrol

Porosity and permeability of tight carbonate reservoir rocks in the north of Iraq

F. Rashid*, P.W.J. Glover, P. Lorinczi, R. Collier, J. Lawrence

School of Earth and Environment, University of Leeds, UK

ARTICLE INFO

Article history:

Received 17 October 2014

Accepted 11 May 2015

Available online 19 May 2015

Keywords:

Tight carbonates

Porosity

Permeability

Reservoir quality

Petrofacies

Kometan Formation

Iraq

Permeability prediction

ABSTRACT

The distribution of reservoir quality in tight carbonates depends primarily upon how diagenetic processes have modified the rock microstructure, leading to significant heterogeneity and anisotropy. The size and connectivity of the pore network may be enhanced by dissolution or reduced by cementation and compaction. In this paper we have examined the factors which affect the distribution of porosity, permeability and reservoir quality in the Turonian–Campanian Kometan Formation, which is a prospective low permeability carbonate reservoir rock in northern Iraq. Our data includes regional stratigraphy, outcrop sections, well logs and core material from 8 wells as well as a large suite of laboratory petrophysical measurements. These data have allowed us to classify the Kometan Formation into three lithological units, two microfacies and three petrofacies. Petrofacies A is characterized by dense and compacted and cemented wackstone/packstone with nanometer size intercrystalline pores and stylolites and presents a poor reservoir quality (porosity range 0.005 ± 0.01 to 0.099 ± 0.01 , permeability range 65 nD–51 μ D). Occasional open fractures in Petrofacies A improve reservoir quality resulting in a 2–3 order of magnitude increase in permeability (up to 9.75 mD). Petrofacies B is a dissolved wackstone/packstone that contains moldic and vuggy pores (porosity range 0.197 ± 0.01 to 0.293 ± 0.01 ; permeability range 0.087–4.1 mD), with both presenting good reservoir quality, while Petrofacies C is a carbonate mudstone that has undergone dissolution and possibly some dolomitization (porosity range 0.123 ± 0.01 to 0.255 ± 0.01 ; permeability range 0.065–5 mD). All three petrofacies can be distinguished from wireline log data using porosity and NMR measurements. A poroperm plot of all of the data is fitted by a power law of the form k (mD) = $a\phi^b$ with $a=28.044$ and $b=2.6504$ with coefficient of determination, $R^2=0.703$. When the permeability is predicted with the RGPZ model of the form k (mD) = $d^2 \phi^{3m} / 4am^2$ with mean grain diameter $d=10 \mu\text{m}$, and mean cementation exponent $m=1.5$ and $a=8/3$ a better fit is possible with $R^2=0.82$.

© 2015 Elsevier B.V. All rights reserved.

1. Introduction

The Middle Turonian to Lower Campanian rock succession in the central part of Iraq is represented by the Khasib, Tanuma and Sa'di Formations (Aqrawi, 1996). These formations host producing fields including the East Baghdad fields in an important reservoir-seal system, which contains an estimated 9 billion barrels of oil in-place (Al-Sakini, 1992; Aqrawi, 1996). The equivalent of the Middle Turonian to Lower Campanian rock succession in North Iraq is the Kometan Formation, which may also be productive where it is sufficiently fractured (Jassim and Goff, 2006). Fig. 1 shows the palaeogeography map of the Kometan Formation and its equivalent rocks in Iraq, while Fig. 2 shows the positions of the various

geological structures, major faults, fields and wells referred to in this paper.

The Kometan Formation is a fractured reservoir unit that produces commercial oil in some oil fields in the north of Iraq (Aqrawi, 1996). The Taq Taq oil field, for example, is a fractured Cretaceous reservoir that includes the Kometan Formation and produces light oil (41 API) with estimated recoverable reserves of 700–750 million barrels. It has been predicted that the field will produce 200,000–250,000 barrels per day when it is fully developed (TTOPCO, 2007).

In the Kirkuk embayment, the Kometan Formation is recognized as a productive formation in the oil reservoirs at the Avanah and Baba Domes of the Kirkuk structure and in the Bai Hassan field, as well as producing gas in the Jambur oil field (Aqrawi et al., 2010).

The equivalent formations in the central and southern parts of Iraq, which are characterized by the chalky units of the Khasib and Sa'di Formations with intercalation of shale and marl of the

* Corresponding author. Tel.: +44 7445291315.
E-mail address: efnr@leeds.ac.uk (F. Rashid).

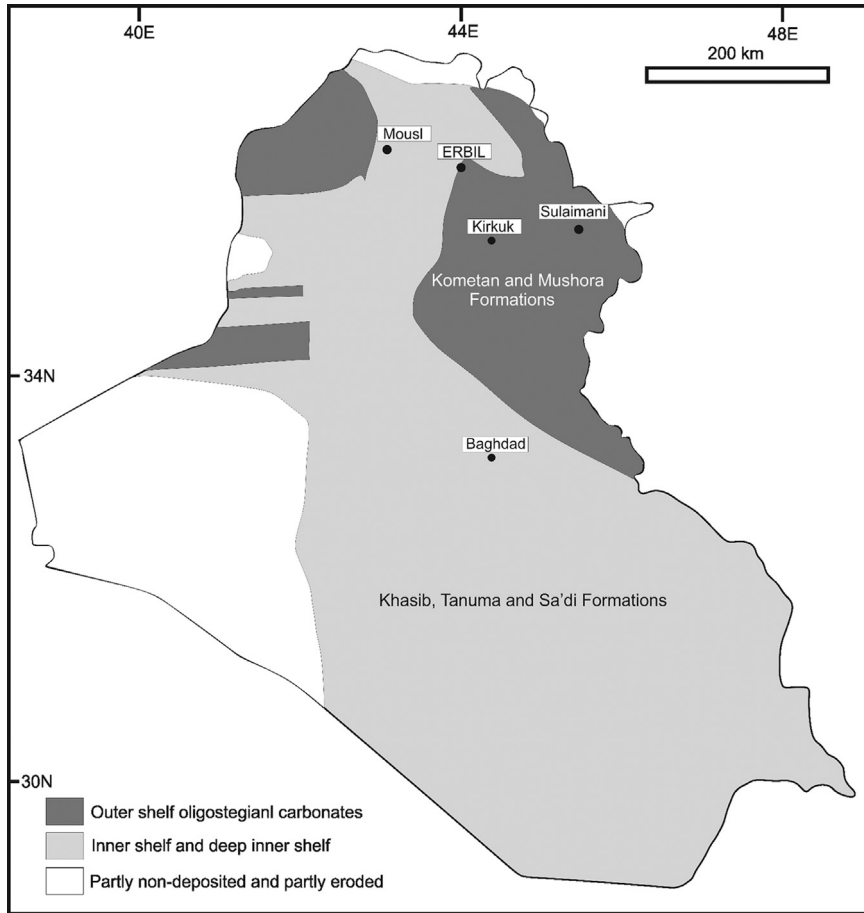


Fig. 1. Palaeogeographical map of the Kometan Formation and its equivalent formation in Iraq (Jassim and Goff, 2006).

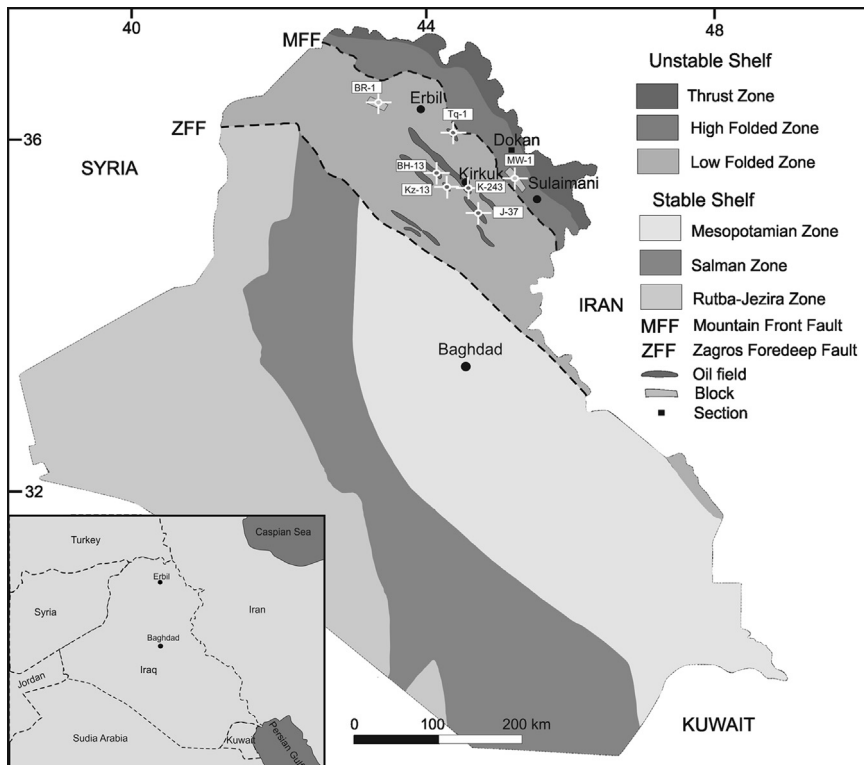


Fig. 2. Tectonic division of Iraq (after Aqrawi et al., 2010), showing the investigation area and including the wells used in this work as well as the position of the Dokan out-crop section.

Tanuma Formation, have porosities in the range 18–23% and permeabilities about 10 mD (Aqrawi, 1996). Aqrawi identified the Khasib and Tanuma Formations in the Mesopotamian basin as good reservoir units thanks to the effects of dissolution diagenesis and tectonic activity. More recently, Sadooni (2004) has pointed out that the presence of a chalky matrix, bioturbation and the creation of micro-fractures all combine to enhance the reservoir properties of the Khasib Formation in central Iraq. Al-Qayim (2010) used previous studies of some of the central oil fields of Iraq to divide the Khasib Formation into four reservoir units. He showed that diagenesis and micro-fracturing enhanced reservoir quality, with high quality being characterized by abundance of moldic, vuggy and intercrystalline porosity with values greater than 20% and permeability in the range 1–25 mD. Garland et al. (2010) have also identified that dolomitization caused local development of porosity in the Kometan Formation. He said that, as one of the Cretaceous targets, high productivity had been achieved from the Kometan Formation, and he has interpreted the reservoir system as a fractured reservoir, where storage and deliverability are only controlled by fracturing.

Currently, there is a lack of publicly available data concerning the evaluation of the Kometan Formation, with most information residing in confidential reports belonging to oil companies working in northern Iraq. The lack of a large amount of good, freely available information about the comet and formation makes it difficult to begin this paper with only a short introduction. Instead we will first introduce the role of the Kometan Formation in the light of the regional geologic and tectonic setting and then move on to how we obtained our data, the results and the inferences that we can make. The heart of this paper considers the lithofacies, porosity, porosity distribution, permeability and the effect of fractures on the petrophysical properties of the Kometan Formation in northern Iraq, in an attempt to assess its reservoir quality and to make these data more widely available in the literature.

2. Regional setting

The Zagros Orogenic Belt (Zagros Mountains), which trends approximately NW–SE through northern Iraq and Iran, was formed during the Cretaceous and Tertiary collision of Arabia and Eurasia, resulting in a range of structures. Presently, the Zagros deformation zone is characterized by strike-slip and contractional movements. These movements result from strain being partitioned into dextral strike-slip movements along mainly NW–SE faults and a shortening component in a NE–SW direction (Vernant et al., 2004). Tectonic evolution during the Early Cretaceous was characterized by discontinuation and termination of the westward motion of the Arabian Plate and central Iranian plates as a result of the opening of the South Atlantic Ocean and the closure of the Palaeo-Tethys, respectively (Iranpanah and Esfandiari, 1979; Sattarzadeh et al., 2000).

In the Cretaceous, the eastern shelf platform of the Arabian Plate was covered by the shallow, neritic, passive margin carbonates and local clastics that represent the Lower Cretaceous reservoir in the Kirkuk Embayment Zone, which includes existing and newly discovered oil fields in Kurdistan. A foreland basin was formed on the northern margin of the Arabian plate during the Turonian–Eocene in response to loading of the crust by a thrust sheet formed as a result of compression on the north-east margin of the Arabian Plate by the Iranian Plate (Jassim and Goff, 2006).

A major event of the Late Cretaceous tectonic history involved the collision of the two continental parts of the Arabian and Iranian plates, followed by the deposition of the Kometan Formation on the north-east margin of the Arabian Plate (Karim and Taha, 2009). Fig. 3 shows the structures at the time of the

deposition of the Kometan Formation. The trench between the two plates was filled with radiolarites and ophiolites slightly before the collision, and these trench materials were uplifted and thrown onto the continental part of the Arabian Plate rising above sea level near the suture zone of the plates. The early Cretaceous rocks that had been deposited on the Arabian Plate, the latest of which was the Qamchuqa Formation, were deformed into a forebulge by the weight of the accretionary prism and thrusting Iranian Plate. The Kometan Formation began to be deposited in the resulting depression, directly on top of the Qamchuqa Formation. Subsidence of the suture zone then continued with the water depth increasing and the Kometan Formation passing through a transitional facies to a deeper marine depositional environment in which planktonic foraminifera and lime muds were deposited as part of the Kometan Formation (Karim and Taha, 2009).

3. The Kometan Formation

Buday (1980) classified the Cretaceous rock units in Iraq into several cycles and sub-cycles based on breaks in the sedimentation process and tectonic activity during the period of deposition. The Turonian to lower Campanian sub-cycle rock units were deposited as a part of a middle Cretaceous rock unit over a huge area in Iraq. The carbonate rock of the outer shelf and basinal Kometan Formation in the north of Iraq is correlated chronostratigraphically with deep inner shelf and lagoonal carbonates and the clastic rock units of the Khasib, Tanuma and Sa'di Formations in central and south Iraq (Aqrawi, 1996).

Sadooni (2004) has stated that the middle Turonian to lower Campanian succession in Iraq is comprised of homogeneous carbonate sediments with a lack of sandstone and evaporites, and includes the Balambo, Dokan, Gulneri and Kometan Formations in Kurdistan and the Khasib, Tanuma and Sa'di Formations in the Mesopotamian Basin.

The Kometan Formation consists of a range of fine grained carbonate lithologies deposited in shallow shelf, restricted settings (oligosteginal facies) to open marine (globigerinal facies) settings (Buday, 1980; Abawi and Mahmood, 2005; Jassim and Goff, 2006). In Kurdistan, the formation is composed entirely of globigerinal and oligosteginal facies, but toward the west and south-west argillaceous facies increase. The deep marine pelagic limestone of the Kometan Formation in Kurdistan and the western part of the Zagros basin changes laterally into the bioturbated chalky limestone, shale and marly limestone of the Khasib Formation, lagoonal shale and carbonate of the Tanuma Formation, and open shelf globigerinal limestone of the Sa'di Formation in the Mesopotamian basin of central Iraq and in south Iraq (Al-Qayim, 2010) as shown in Fig. 4.

According to van Bellen et al. (1959) and Dunnington (1958), the Cretaceous carbonate rocks of the Kometan Formation were first recognized in 1953 by Dunnington at Kometan Village near Endezah, north-east of the town of Rania near the city of Sulaimani, which is close to the contact between the Balambo Tanjero Zone and the High Folded Zone in the Kurdistan region of Iraq. In the type locality, the Kometan Formation is described as 36 m of white weathered, light grey, thin and well-bedded globigerinal–oligosteginal limestones. It is locally silicified with chert nodule concentrations in occasional beds, and glauconitic horizons, especially at the base of the Kometan Formation.

This formation was subsequently identified in a wide range of localities in the Imbricated Zone, High Folded Zone and in the Low Folded Zone, in outcrop and sub-surface sections. The Kometan Formation can be distinguished lithologically from other Cretaceous successions in outcrops of the area and in the Low Folded Zone wells. It becomes marly toward the west and south-west of

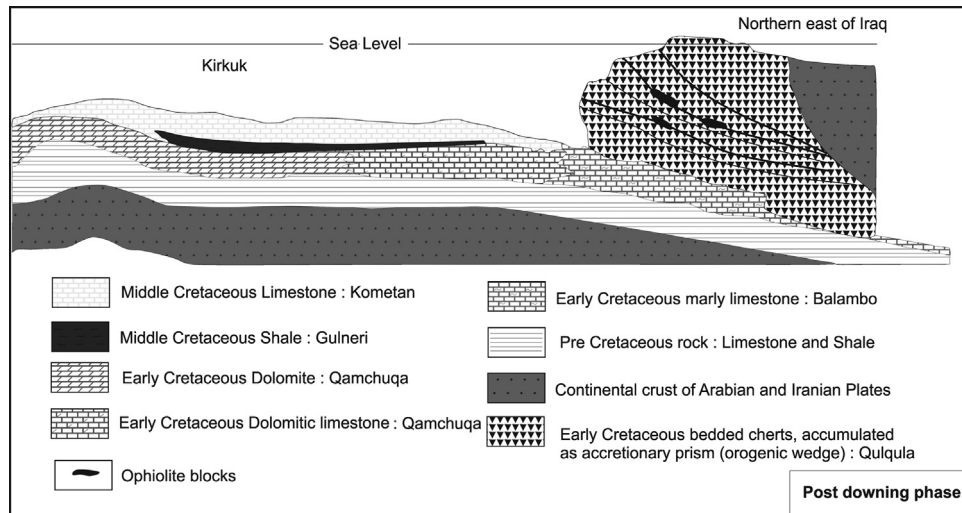


Fig. 3. Tectonic evolution of the north-east margin of the Arabian Plate (after Karim and Taha, 2009), where the terminology ‘post downing’ used by these authors refers to the situation after subsidence has occurred.

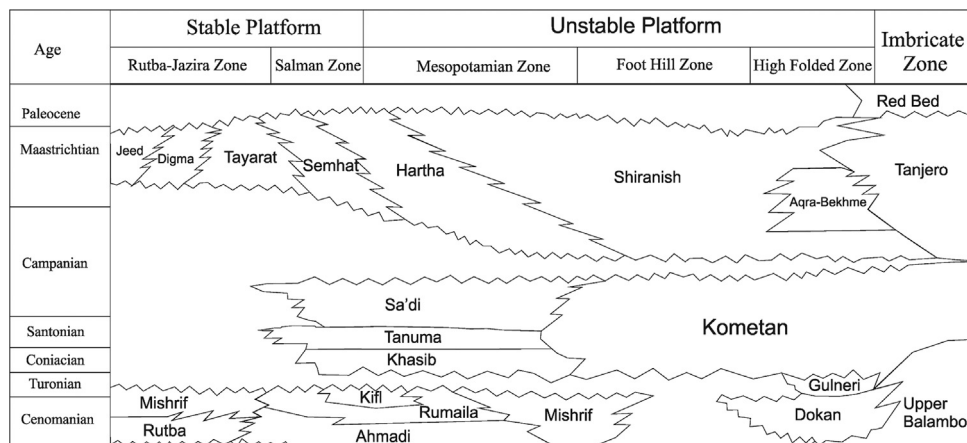


Fig. 4. Chronostratigraphic division of Cretaceous rock in Iraq (Al-Qayim, 2010).

Iraq (van Bellen et al., 1959; Dunnington, 1958), and its biofacies changes laterally from a mixture of globigerinal limestone and oligosteginal intercalation to oligosteginal facies (Buday, 1980).

The thickness of this carbonate rock unit is variable, varying from its type section to the surrounding area and different tectonic zones of Kurdistan, and in the north-east of Iraq even in the same tectonic division. In general it has a variable thickness up to 100–120 m but “averages 40–60 m” (Buday, 1980). Its thickness is about 105 m in the Dokan section; 78 km south-west of Sulaimani, and 110 m in the Taq Taq Oil Field. Its thickness increases again toward the Kirkuk embayment, and it reaches 120 m in well K-109 and 178 m in K-116 of the Kirkuk Oil Field. However, the thickness is 145 m in CH-2 of the Chamchamal Field, which is 60 km south-west of Sulaimani and 50 km north-east of Kirkuk.

Upper Cenomanian oligosteginal facies of the Balambo Formation underlie the Komatan Formation unconformably, but with a lack of angular discordance. Buday (1980) recognized unconformable lower contacts of the Komatan Formation with both the Cenomanian Dokan, Albian Upper Qamchuqa and Turonian Gulneri Formations, while Kaddouri (1982) has shown conformable contact between the base of the marly silty glauconitic limestone of the Komatan Formation and the pebbly, sandy detrital limestone of the Tel Hajar Formation. Jassim and Goff (2006) have also confirmed that the lower contacts of the Komatan Formation with the underlying Albian–Cenomanian Formations in the area are unconformable.

The Shiranish Formation overlies the Komatan Formation, again with an unconformable contact, but without angular discordance. A glauconitic deposit exists at the base of the Shiranish Formation and can be used as a marker bed (van Bellen et al., 1959; Dunnington, 1958). The contact occasionally appears conformable (Buday, 1980) or as a disconformity (Jassim and Goff, 2006).

4. Materials and methods

The data used in this paper have two different provenances.

Provenance 1. Data and rock samples from the Kurdistan Region, which encompasses the Dokan outcrop, 80 km north-east of Sulaimani city. In this area the Komatan Formation is most complete and has well-differentiated boundaries. This group of data and samples also covers the Miran West exploration license, located 12 km west of Sulaimani, and the Taq Taq field, which is located in the Zagros Folded Thrust Belt within the Kirkuk Embayment. The Taq Taq anticline lies in the folded foothills to the southwest of the Mountain Front Fault, which separates the High Zagros Mountains from the Kirkuk Embayment and about 60 km north-east of the Kirkuk oil field. This group also contains the Barda Rash exploration license in the Low Folded Zone toward the northern margin of the investigated area, and about 20 km south-west of the city of Erbil.

Provenance 2. The second group is defined as that data provided by the North Oil Company, which covers the Kirkuk embayment of the Low Folded Zone, and includes the Kirkuk, Khabaz, Bai Hassan and Jambur fields in the city of Kirkuk, north-east of Iraq. The Kirkuk oil field is located geographically in the centre of Kirkuk and tectonically is part of the Kirkuk embayment of the Zagros Folded Thrust Belt. The Khabaz anticline is one of the Kirkuk embayment structures located 23 km south-west of Kirkuk city, with relatively minor surface expression by comparison to the adjacent Bai Hassan, Jambur and Kirkuk anticlines. The Bai Hassan field is located in Kirkuk city, trending north-west to south-east and parallel to the Kirkuk field and 20 km to its south-western side. The Jambur field is located south-east of Kirkuk.

The material that we have gathered for analysis in this paper includes 173 core plug samples representing 99 m of core from various wells and 95 m of whole outcrop in the Dokan area. These core samples were used in a range of laboratory petrophysical and petrographical tests. Petrophysical wireline data from seven wells were also analyzed. In addition, we used some existing petrophysical measurements that had been made previously by the research department of the North Oil Company. The research materials are summarized in Table 1.

Approximately 55 core plug samples were provided from 5 wells (Table 1) by the North Oil Company-Kirkuk, while a further set of samples from the Dokan outcrop, which we took during a field campaign, provided a further 70 core plugs. All core plugs were nominally 1.5 in. in diameter and 2 in. long, cleaned and dried under vacuum at 60 °C for 48 h. Gamma ray and XRD measurements on core plug end cuttings indicated very low clay content, implying that drying at 60 °C would not substantially alter the microstructure of the core plugs. Routine core analysis was carried out. Since the conventional steady-state method for determining permeability of very low permeability samples (< 1 mD) is difficult and takes a very long time, selected plug samples were measured using a pulse-decay approach with a 700 psig (4.82 MPa) confining pressure (Jones, 1997). Nuclear magnetic resonance spectroscopy was also carried out on a selection of samples in the laboratory, and it was found that this data was helpful in distinguishing between the petrofacies, which we have defined for the Kometan Formation.

A total of 25 samples were prepared from core plug cuttings after impregnation with a fluorescent blue resin in order to highlight porosity during the procedure for measuring porosity

by image analysis of photomicrographs. The visit was also useful for holding together poorly consolidated and/or fractured samples. Samples were also stained for carbonate identification. Bulk rock X-Ray diffraction analysis was carried out to indicate the existence and relative abundance of crystalline phases within the selected samples. A high-resolution SEM (High resolution field emission scanning electron microscope) with magnifications of 1:10,000 and 1:20,000 were used for the identification of pore types. However, since the samples have a highly cemented fabric, achieving a clear pore image was often difficult.

The litho-facies, porosity, permeability and reservoir potential have been obtained by synthesizing data from observation of hand specimens in the field together with visible and scanning electron microscopy, XRD analysis, porosity and permeability measurement on material collected from the field or from cores. Well log analysis has allowed us to make measurements on the Kometan Formation underground at a range of scales, which also help us to understand its structure, origin and evolution. In this section we describe the varied lithology of the rocks that make up the Kometan Formation before looking in more detail at the microfacies they contain. The measured porosity and permeability of the rocks will then be discussed briefly, before combining all the previous observations and test results in order to define three petrofacies that describe the rocks of the Kometan Formation, and which represent different degrees of reservoir potential.

4.1. Lithofacies and microfacies

4.1.1. Lithofacies

The lithofacies of the Kometan Formation were examined by carrying out an integrated stratigraphic and sedimentological analysis of a complete and well-exposed section of the Kometan Formation in an outcrop at Dokan, 80 km north-west of Sulaimani city, supported by core data and cutting samples from the wells listed in Table 1. The analysis considered sedimentary texture, including lithology, color, sedimentary structure, evidence of diagenesis, the Dunham microfacies classification (Dunham, 1962), observation of pore structures, and the presence and distribution of fractures and stylolites. The interpreted results were compared with the gamma ray log from each of the wells in order to understand the variation of shaliness within the formation.

Initially, thin section petrography was carried out on 25 samples to obtain information about their composition, pore type, texture and evidence of diagenesis. Subsequently, 10 samples were

Table 1
Material and data.

Location	Well	Core length (m)	Cuttings samples	Core plugs	Core measurements carried out	Well logs	Geological section
Dokan outcrop	–	95		70	Porosity, permeability, NMR, capillary pressure, SEM, XRD, thin section		Yes
Taq Taq Field	Tq-1	18	70	15	Porosity, permeability, NMR, capillary pressure, SEM, XRD, thin section	GR, DRHO, NPHI, Sonic	Yes
Kirkuk field	K-243	18	20	15	Porosity, permeability, NMR, capillary pressure, SEM, XRD, thin section	GR, DRHO, NPHI, Sonic	Yes
Jambur field	J-37	18	27	15	Porosity, permeability, NMR, capillary pressure, SEM, XRD, thin section	GR, DRHO, NPHI, Sonic	Yes
Bai Hassan field	BH-13	36	25	5	Porosity, permeability, NMR, capillary pressure, SEM, XRD, thin section	GR, DRHO, NPHI, Sonic	Yes
Khabaz field	Kz-13	9	12	5	Porosity, permeability, NMR, capillary pressure, SEM, XRD, thin section	GR, DRHO, NPHI, Sonic	Yes
Miran West	MW-1		20			GR, DRHO, NPHI, Sonic	Yes
Barda Rash	BR-1		5			GR, DRHO, NPHI, Sonic	Yes

chosen to be analyzed using a scanning electron microscope, in order to identify pore types and the nature of pore preservation. In a further analysis, 16 samples were selected for X-Ray diffractometry (XRD), to obtain detailed information about the clay fraction of each sample and its bulk rock mineralogy. The clay composition data was especially important for the samples from the Dokan outcrop, so that the variation of shaliness in the outcrop section could be compared with that from the gamma ray well log data. All of the samples were also submitted to Nuclear Magnetic Resonance Spectrometry in the laboratory. This data provides a spectrum of T_2 relaxation times which indicate the size of fluid-filled pores and the mobility of fluids in those pores. We found that the T_2 relaxation time spectra were useful in distinguishing between rocks from Petrofacies B and Petrofacies C.

We have found that the Kometan Formation can be divided into two main lithologic units; an Upper unit (K1) and Lower unit (K2), depending on lithology variation, biofacies and gamma ray log values. This stratigraphic subdivision is interrupted in some parts of the study area by the deposition of a shaly limestone unit (Ksh). The shaly limestone unit is present throughout the western margin of the Kirkuk embayment, as shown in Fig. 5 and several succeeding figures. Figs. 6 and 7 show correlated gamma ray logs with interpreted lithologies for the Kometan Formation on a NW–SW and N–SE section, respectively. Figs. 8 and 9 show optical photomicrographs of selected samples either stained with alizarin red or impregnated with blue resin and then viewed under polarized light, respectively.

4.1.2. The Upper Unit of the Kometan Formation (K1)

The upper unit of the Kometan Formation (K1) is characterized by light gray to white chalky, microcrystalline, hard, homogeneous, well-bedded limestone of globigerinal limestone facies. It is highly stylolitic, especially within the core samples from the Tq-1,

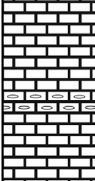
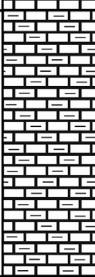
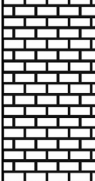
Age	Formation	Lithology	Description
Campanian	Upper Unit (K1)		Light gray, white, chalky, well-bedded globigerinal limestone. Local silicified with chert nodules deposited along bedding planes (example shown). The limestone beds are highly jointed and fractured which enhances the reservoir quality. Stylolites are observed throughout the Dokan section, Taq Taq, Kirkuk, and Jambur fields. Stylolites filled with clay, calcites, pyrite and occasionally bitumen. Observed pores are partially or totally filled with cement.
	Shaly LMST Unit (Ksh)		Shaly limestone unit characterised by the intercalation of bands of thin, fissile, dark shale and light grey limestone. This unit is recorded in the Khurmala and Avana domes of the Kirkuk field and extends towards the south-west of the Kirkuk embayment zone including the Bai Hassan and Khabaz fields.
Turonian	Lower Unit (K2)		Light gray to dark gray globigerinal limestone. Highly stylolitic with fractured beds. The upper part of this unit is intercalated with light brown oligosteginal limestone facies. Pores are filled with cement.

Fig. 5. Summary of the stratigraphy and lithology of the Kometan Formation in the study area, derived from field observations, analysis of cores and cuttings, and log measurements.

K-143, and J-37 wells, and in the Dokan outcrop. No macroscopically obvious porosity was recorded even on the surface of the plug samples in these wells, or at the outcrop. Some of the stylolite surfaces were filled with residual bitumen. Stylolites were found to be very rare or absent in core samples from the BH-13 and Kz-13 wells. The K1 unit is highly fractured in a near vertical direction. The fractures were either partially filled with calcite cement, or occasionally remained open with clean fracture surfaces.

There are also beds of flint within the limestone beds of the Upper Unit in the Dokan outcrop section and also in core samples from well BH-13. The limestone beds in the Bai Hassan field are slightly porous and contained tight, nearly vertical fractures some of which were filled with secondary calcite. Oil staining, which caused core samples to appear greasy light brown, was recorded over a 65 m thick interval from top of the K1 unit, and was very abundant in the Kirkuk and Taq Taq oil field cores.

The thickness of the K1 unit varied throughout the studied area; and was measured to be 68 m thick at the Dokan outcrop, and 62 m thick in well Tq-1 of the Taq Taq field. The thickness of the K1 unit was observed to increase toward the north-east of the investigation area, reaching 114 m in the Miran West block and 115 m in the Jambur field. The thickness of the unit also increases toward the south and south-west of the Kirkuk embayment, with a thickness of 78.5 m being recorded in well K-243 of the Kirkuk field, 125.5 m in well BH-13 of the Bai Hassan field, and 79.5 m in well Kz-13 of the Khabaz field. By contrast, toward the north-west the K1 unit is completely absent, as exemplified by well BR-1 of the Barda Rash license area. Figs. 6 and 7 show how the K1 unit correlates between the wells analyzed in this paper, while Fig. 2 shows the relative positions of the wells and the sections shown in Figs. 6 and 7.

The upper boundary of the K1 unit is overlaid by marl and marly limestone of the Shiranish Formation at the Dokan outcrop and in all the wells with an exception of wells in the Barda Rash license block, in which the Bekhme Formation replaces the Shiranish Formation.

The lower boundary of the K1 unit is marked with a 2 m thick layer of glauconite. This bed was observed initially in cuttings samples in the Tq-1, K-243, and J-37 wells. There is also evidence for the glauconite bed in the gamma ray logs of most of the wells analyzed, providing a localized peak in the gamma ray log as seen in Figs. 6 and 7. The glauconite bed is an extremely good marker bed indicating the boundary between the Upper Kometan (K1) and Lower Kometan (K2) units in the wells, but was not recorded in the Dokan outcrop section.

4.1.3. The Lower Unit of the Kometan Formation (K2)

The Lower Unit of the Kometan Formation (K2) is also characterized by globigerinal limestone facies, as shown in Figs. 6 and 7, and is composed of hard, massive, light brown to pale brown limestone. Unlike the K1 unit, the globigerinal limestone of the K2 unit is commonly intercalated with bands of oligosteginal facies (Figs. 8, Part D and 9, Part F), which are highly fossiliferous with no visible pores. The limestone beds of the K2 unit are generally highly stylolitic and fractured, as observed in the Dokan outcrop section and Khabaz field core sample.

The K2 unit was recorded in all analyzed wells and at the Dokan outcrop. The top of the K2 unit is immediately below the glauconite bed in the Taq Taq, Miran West, Kirkuk, Jambur and Barda Rash wells. In the Dokan outcrop section the glauconite band was missing, but the top of the unit could be recognized by a band of oligosteginal limestone.

The thickness of the K2 unit is similar throughout the entire studied area; 27 m at the Dokan outcrop and 26.4 m in well Tq-1. Toward the northern extremity of our study, in the Jambur field,

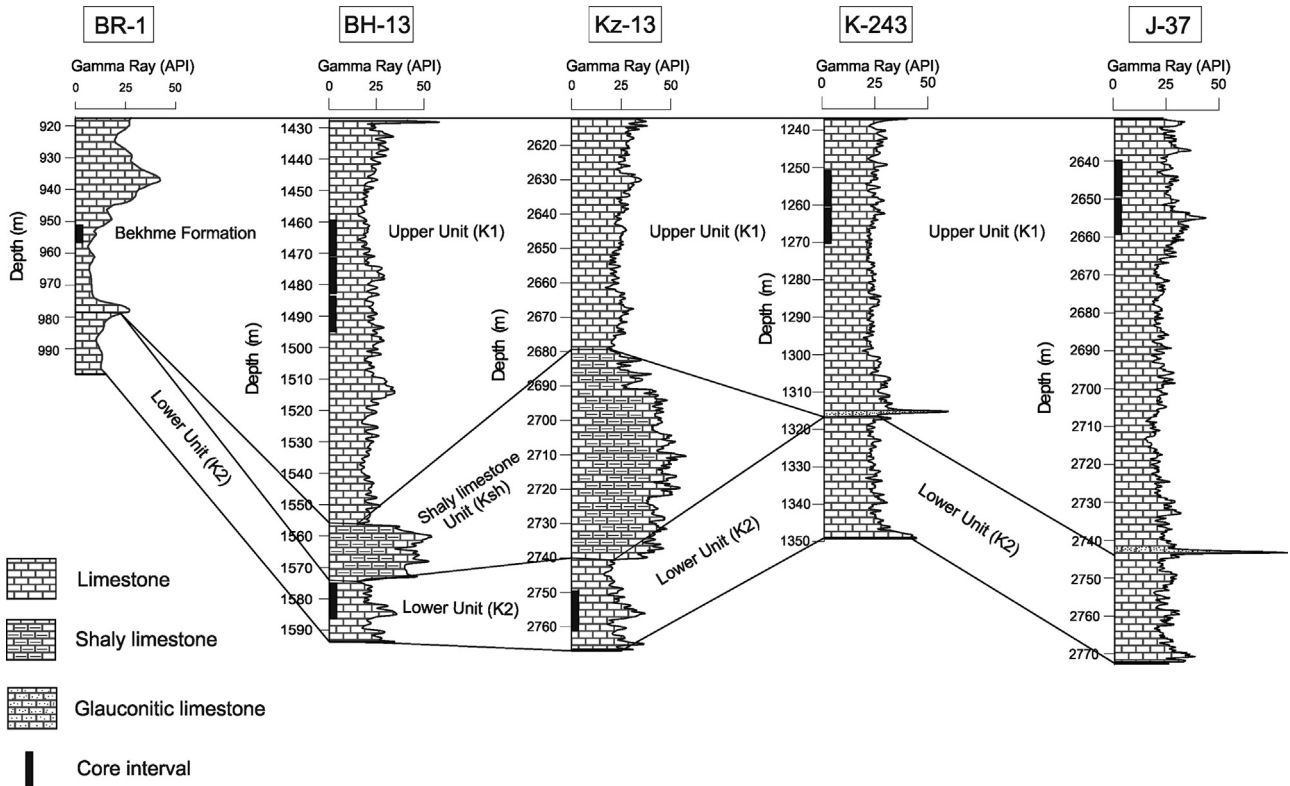


Fig. 6. Correlated gamma ray logs with interpreted lithologies for the Kometan Formation on a NW-SW section incorporating wells in the Barda Rash Block (BR-1), as well as in the Bai Hassan (BH-13), Khabaz (Kz-13), Kirkuk (K-243), and Jambur (J-37) fields.

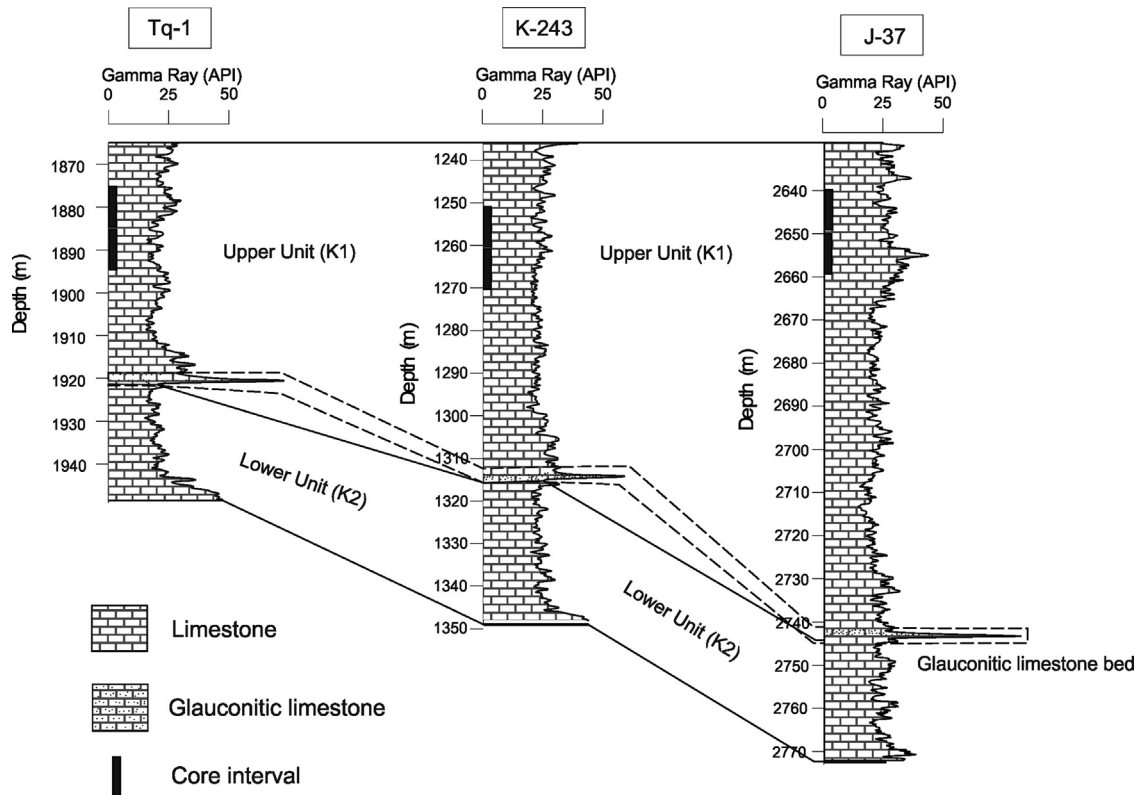


Fig. 7. Correlated gamma ray logs with interpreted lithologies for the Kometan Formation on a N-SE section incorporating wells in the Taq Taq (Tq-1), Kirkuk (K-243), and Jambur (J-37) fields. The deflection of gamma ray caused by the glauconite band that indicates the boundary between Upper (K1) and Lower (K2) units is clearly seen.

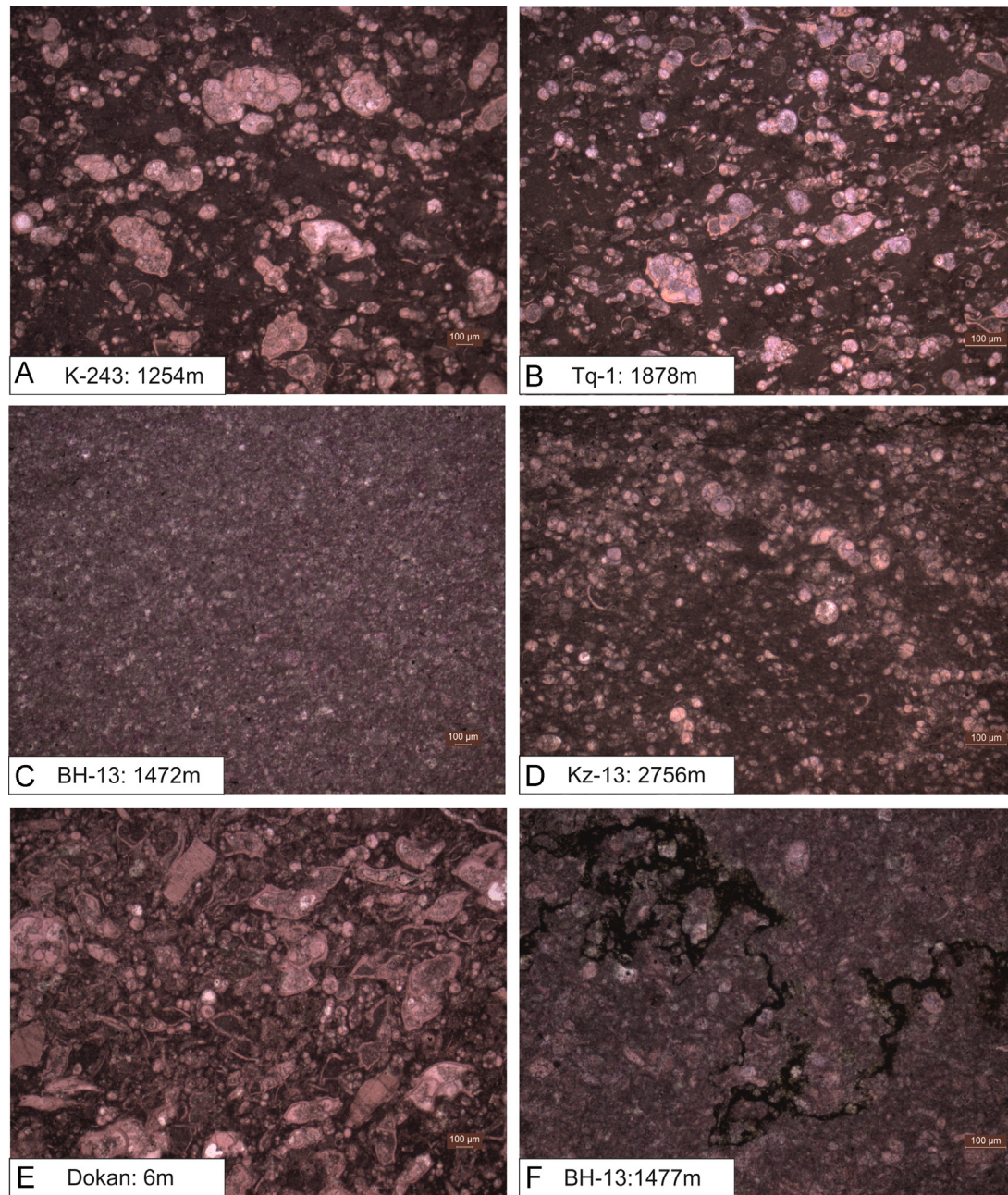


Fig. 8. Photomicrographs of selected samples stained with alizarin red. (A) Wackstone microfacies in Kirkuk field: chambers of foraminifera filled with calcite cement. (B) Wackstone microfacies in the Taq Taq field: highly cemented foraminifera chambers. (C) Mudstone microfacies in the Bai Hassan field. (D) Wackstone microfacies in the Khabaz field: oligosteginal assemblage. (E) Packstone microfacies in the Lower unit (K2) in Dokan section. (F) Wackstone microfacies in the Bai Hassan field, the foraminifera chambers are blocked by cement from stylolitization, and the stylolite is filled with residual oil.

K2 reached 27.2 m in thickness, while its maximum thickness occurs in the Kirkuk embayment; a thickness of 32.1 m was recorded in well K-243. Toward the western margin of the study area the thickness of the K2 unit is 20.6 m in well BH-13 and 26.4 m in well Kz-13. The Kometan Formation consists only of the K2 unit in the Barda Rash license area wells because the Upper (K1) unit is missing. Here the K2 unit, and hence the whole of the Kometan Formation is 20 m thick (Figs. 6 and 7).

A length of 9 m of core was taken from this unit in well Kz-13 of the Khabaz field. The limestone beds were completely saturated with oil and the beds were partially broken as a result of highly inclined and nearly vertical fractures. Such a rock structure might provide a good potential reservoir rock.

4.1.4. The shaly limestone unit of the Kometan Formation (Ksh)

The shaly limestone unit (Ksh) was recorded only in the Bai Hassan and Khabaz fields (Fig. 6). This unit is called 'the Shale Unit' locally, even though the shale volume that has been calculated from the gamma ray log does not exceed 60% in the whole unit. This unit is characterized by grey and black fissile, fine-grained shale, intercalated with argillaceous limestone beds. The rocks of this unit are rarely pyritic, and glauconitic layers are observed particularly at the bottom of the unit allowing us to correlate it with glauconite beds at the bottom of the K1 unit in the Taq Taq, Kirkuk, Jambur and Miran West wells.

Examination of cores and cuttings, as well as log data (see Table 1), has confirmed that our lithological classification of the

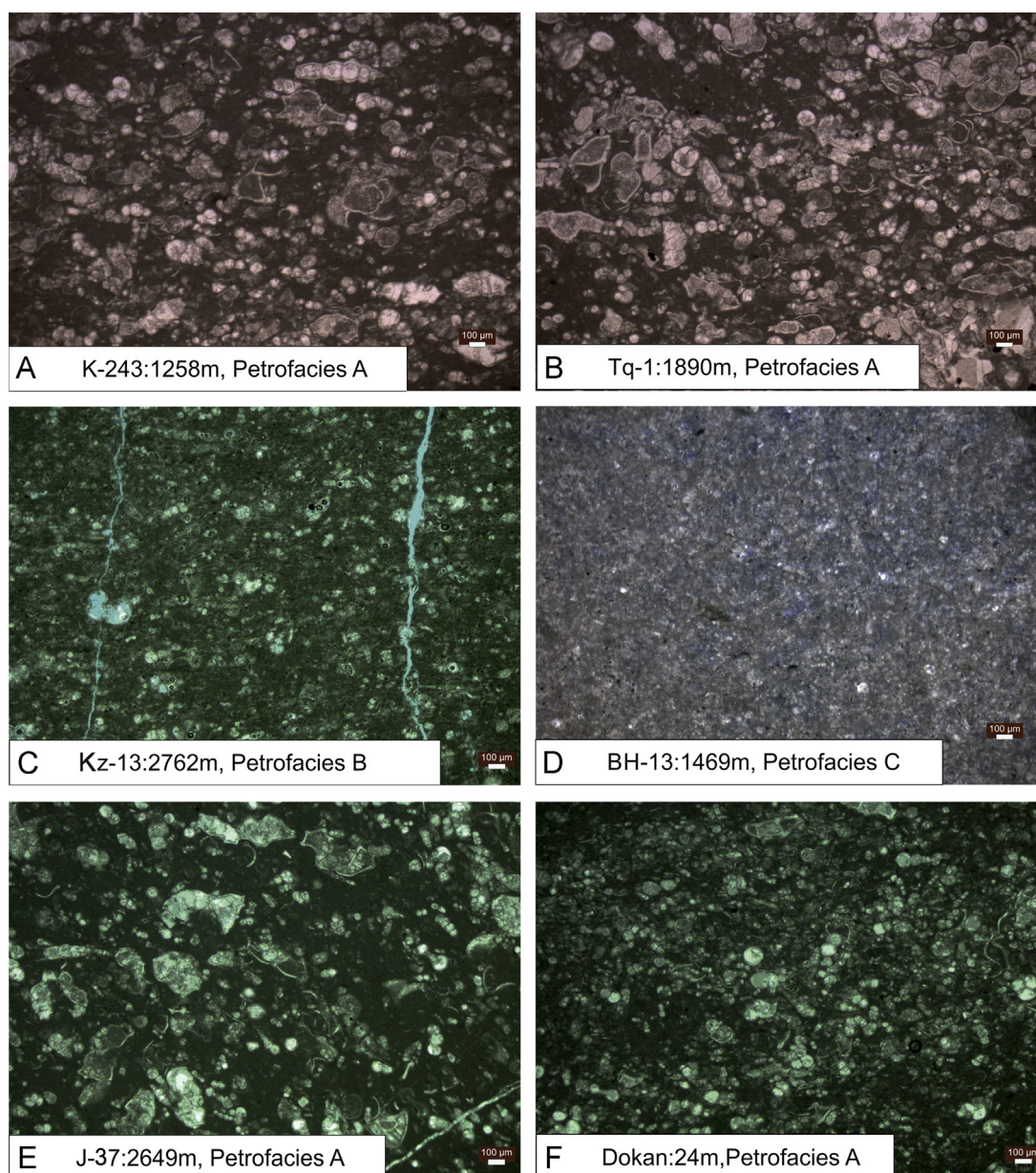


Fig. 9. Photomicrographs of selected samples impregnated with blue resin in plane polarized light. (A) and (B) No pores visible. (C) Moldic pores of foraminifera chambers and open fractures. (D) Highly intercrystalline pores. (D) Moldic pores of foraminifera chambers and open fractures. (E) No visible pores, microfractures filled with calcite cement. (F) Pores totally blocked by cement (lower part of Kometan in the Dokan section).

Kometan Formation throughout the area of investigation can also be applied to all wells, to the Dokan outcrop section, to producing fields such as the Taq Taq, Kirkuk, Jambur, Bai Hassan and Khabaz fields, as well as to exploratory wells in the Miran West license block.

The Barda Rash license block covers an area in the north-west of the studied area (i.e., north-east Iraq). In this license area the Kometan Formation is called the Kometan/Bekhme Formation, and the Komet Company has recognized that the formation shares the same general lithological characteristics as elsewhere in north-east Iraq, but is locally dolomitized. This lithological succession is modified toward the Kirkuk and surrounding fields (Bai Hassan and Khabaz) by dynamic alteration of the stratigraphic position of the shale layers, which are characterized by thin, dark, fissile shale intercalating with the limestone of the Kometan Formation in the middle unit. Abundant chert has been observed in the Bai Hassan field. It is in the form of nodules and irregular chert bands, and presents a very similar style to our Dokan outcrop section in

Kurdistan. It is, so far, the only example of significant chert to be observed in producing or exploratory wells that penetrate the Kometan Formation in north-east Iraq.

4.1.5. Microfacies

The Kometan Formation samples are dominated by diverse assemblages of planktonic foraminifera. Globogerinoid assemblages characterize the Upper (K1) and Lower (K2) units, while oligostigenoid assemblages are only found in the Lower (K2) unit. The sediments of the Kometan Formation have been described as bioturbated planktonic foraminiferal wackstone/packstones and mudstones by Dunham (1962). The fauna present indicate that the Kometan sediments are largely planktonic in origin and were deposited in a fairly deep middle to outer shelf environment under normal marine conditions.

The wackstone/packstone microfacies is very common in the core samples studied in this work, extending from the top to the

bottom of the Kometan Formation in the Dokan outcrop section, as well as wells in the Taq Taq, Kirkuk, Khabaz, Bai Hassan and Jambur oil fields. It is characterized by well-preserved planktonic foraminiferal assemblages, keeled planktonic foraminifera and a lime mud matrix. Fig. 8(parts A, B and E) shows typical assemblages under photomicrography. The XRD analysis and alizarin red dye technique that was used for carbonate identification indicated that the composition of this microfacies is predominantly calcium carbonate (> 90%) and that there is no evidence of dolomitization having occurred. The chambers of the planktonic foraminifera are mostly cemented with non-ferroan calcite, and occasionally filled with pyrite. The diagenetic features in this microfacies are cementation and compaction that together destroyed the reservoir quality of the Kometan Formation after deposition.

The mudstone microfacies is recorded in the Upper (K1) unit of the Kometan Formation, but only in the Bai Hassan and Khabaz fields of the Kirkuk embayment of the Low Folded Zone. This microfacies is characterized by preserved planktonic foraminifera within a significant proportion of lime mud matrix (Fig. 8, Part C). Two samples were analyzed by XRD, showing that the microfacies is composed mainly of calcite (> 90%) with a small amount of dolomite (4–7%). However, the petrographic study of the selected samples did not show any evidence of dolomitization when using alizarin red as a calcite indicator. The chambers of the planktonic foraminifera were commonly filled with calcite cement, though some partial filling was also noted. Fig. 8(Part F) shows a typical wackstone microfacies in the Bai Hassan field. In this photomicrograph the foraminifera chambers are blocked

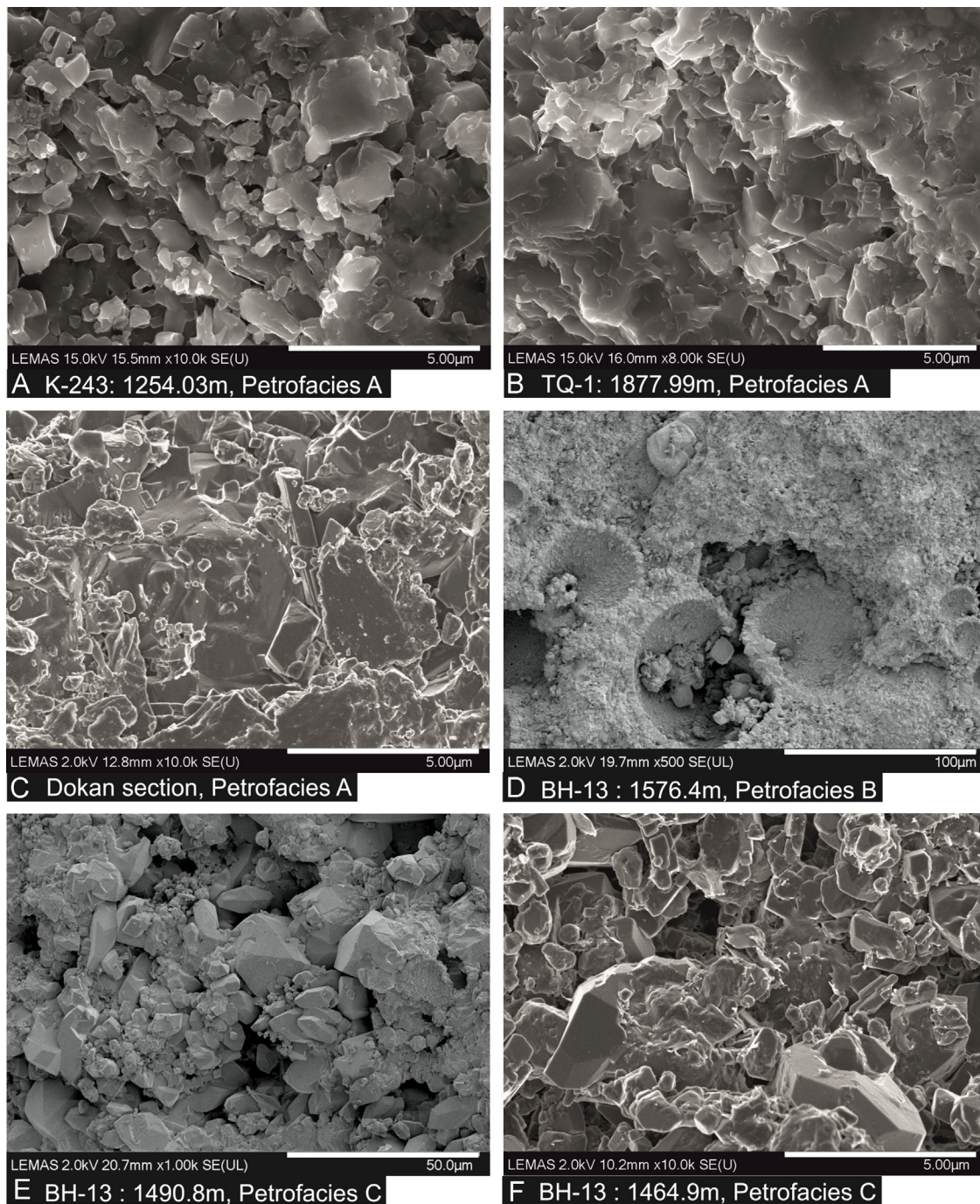


Fig. 10. High resolution scanning electron photomicrographs of selected samples: A–C for Petrofacies A; D for Petrofacies B; C, E and F for Petrofacies C.

by cement as a result of the formation of stylolites, which here are filled with residual oil.

4.2. Porosity, permeability and petrofacies

4.2.1. Porosity

Most carbonate rocks are frequently characterized by multiple-porosity systems that impart petrophysical heterogeneity to reservoir rocks (Mazzullo and Chilingarian, 1992). Consequently, the value of porosity, the porosity type, and porosity distribution often govern the production values and simulation characteristics of the gross carbonate reservoir interval (Wardlaw, 1996).

In carbonates, the pores are commonly classified into two groups according to their origin (Choquette and Pray, 1970). Primary pores or depositional porosity are pores, which are formed as the sediment is deposited. Primary porosity includes interparticle, intraparticle, fenestral, shelter and growth framework pores. Secondary porosity is that porosity that is formed as a result of post-depositional changes to the rock by diagenetic processes, and often includes both dissolution and cementation. It should be noted that an initial pore with a primary porosity may be enlarged by dissolution or reduced in volume by cementation to give a secondary porosity. Hence, the classification refers to the overall porosity of the rock rather than the type of each pore. However, certain pores may be created solely by secondary diagenetic processes.

Primary porosity in carbonate rocks is commonly reduced extensively by the effect of cementation and compaction during post-depositional burial, such that most pore types in carbonates are of secondary origin (Halley and Schmoker, 1983; Mazzullo and Chilingarian, 1992). The exceptions are those primary pores that are preserved as a result of hydrocarbon accumulation within the pores early in the rock's history (Feazel and Schatzinger, 1985).

The porosity of the Kometan Formation has been studied both in the field and in the laboratory. In the field, we have classified the porosity according to the classification of Choquette and Pray (1970) for carbonate rocks that takes account of pore morphology and the origin of the pore volume. Visible moldic and intercrystalline pores were observed within the broken fresh surfaces of all samples, and most of them were filled with calcite cement. Stylolitization and fracturing were sometimes highly developed in the samples and were sometimes missing. Different types of fractures including micro-fractures, open fractures, closed fractures, and partially cemented fractures were all identified. Some of these fractures may enhance fluid flow, while others may act as a barrier to the reservoir fluids. Fractures, which are inclined, nearly vertical, and which cross-cut stylolites, were all observed in the outcrop section and also in the core samples.

In the laboratory, a petrographic study of thin-sections under plane and polarized light on samples, which had been impregnated with a fluorescent blue resin (Fig. 9), was of limited use because the extremely small pores were often not visible even at the highest magnifications. Instead, a high resolution scanning electron microscope was used for the identification of pore types, showing that intergranular and moldic pores were the most common types of pore in the Kometan Formation (Fig. 10).

In total, helium porosity measurements were made on 125 core plugs, while a further 50 core plug samples were measured by the North Oil Company. The combination of these data shows that the Kometan Formation is composed of rocks, which have porosities that range from very low values (0.02 ± 0.01) to rather high values (0.35 ± 0.01). The distribution of porosity values is shown in Fig. 11, which is grouped into three distinct petrofacies (A, B and C) that can be recognized from the petrophysical measurements of the rock samples in the laboratory, although only Petrofacies A may be separated from the other two on the basis of porosity alone.

4.2.2. Permeability

We have carried out 125 pulse decay measurements of the permeability of our Kometan samples. In addition, we have analyzed a further 50 steady-state permeability measurements on core plugs that had already been carried out by the North Oil Company. When combined, these measurements range from 65 nD ($6.42 \times 10^{-20} \text{ m}^2$) to 9.75 mD ($9.62 \times 10^{-15} \text{ m}^2$). This range of permeability clearly classifies the Kometan Formation as a tight carbonate reservoir. The distribution of permeabilities (Fig. 12) mirrors that of the porosity but with a greater degree of overlap between the permeability populations for each petrofacies. The overlap results from the enhancement of the permeability of some low porosity and permeability samples from Petrofacies A by open fractures.

4.2.3. Petrofacies

In this study we define a petrofacies as a classification of a rock type based on its microfacies, but also taking account of the value of its porosity, the type and origin of the pores it contains, its permeability, and any other distinguishing diagenetic features that may be quantified petrophysically.

We have recognized three types of petrofacies in the Kometan Formation. Figs. 11 and 12 show the distribution of the measured porosities and permeabilities for each petrofacies, while Fig. 10 shows typical electronphotomicrographs for each type.

4.2.3.1. Petrofacies A.. This petrofacies is defined from the wackstone/packstone microfacies of the globigerinal and oligosteginal limestone,

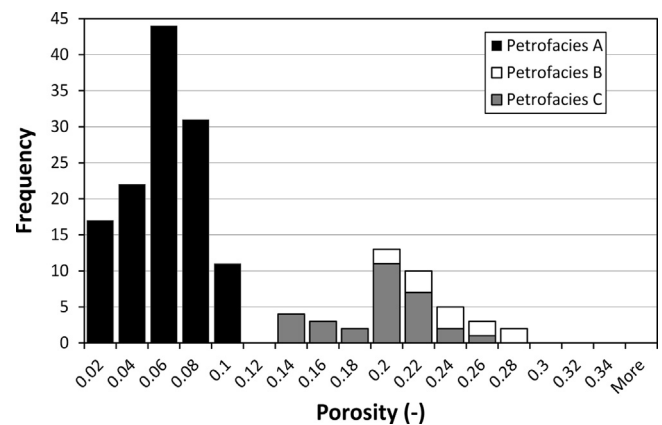


Fig. 11. Stacked histogram of the porosity for each of the three petrofacies.

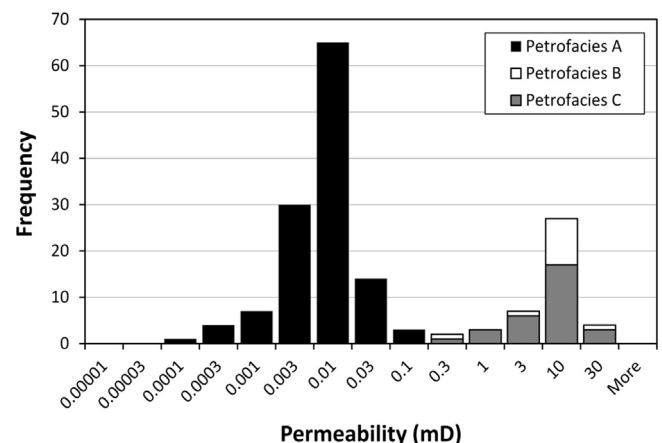


Fig. 12. Stacked histogram of the permeability (on a logarithmic scale) for each of the three petrofacies.

and is common throughout the sample set, i.e., from the lower part of the Kometan Formation (K1) to its upper part (K2), and covering the entire area studied from the Dokan section to wells Tq-1, K-243, and J-37. It is characterized by well-preserved foraminifera with highly cemented chambers and lime micrite (Fig. 9, parts A, B and F). However, even though the percentage of foraminifera grains exceed 10%, no porosity is visible by eye in either core plugs or in thin-sections. In addition, most fractures are filled by calcite cement (Fig. 9, Part E), which limits the enhancement of fluid flow by fractures, leaving only the partial-filled calcite fractures and intercrystalline pores as pathways for fluid flow.

Microscope study of thin sections by visible polarized light does not show the bluish hue that would identify micro-porosity under the microscope. While, imaging using a high resolution scanning electronic microscope shows intercrystalline pores between calcite crystals, which are of nanometre scale (Fig. 10, parts A–C). The XRD results show that this petrofacies is clean with the percentage of clay minerals not exceeding 4%. All original fabrics of Petrofacies A, including foraminifera chambers, were commonly tightly filled by cement that destroyed macropores and preserved the fabric as a non-porous medium. The porosity of this Petrofacies A ranges from 0.005 ± 0.01 to 0.099 ± 0.01 , while unfractured examples have permeabilities less than 0.1 mD.

The dissolution of carbonate matrix along lines of weakness such as bed boundaries and stylolite surfaces has resulted from deep burial and compaction. This has occurred where material which had been dissolved at points where the pressure is extremely high, due, for example, to interacting asperities, has been carried by flow to be deposited at the closest point where the effective pressure is less (Ramsay and Huber 1983; Rowland et al., 2007).

The matrix of Petrofacies A was deposited with a high primary porosity at an early stage of deposition (eogenetic stage), and has undergone post-depositional diagenesis including dewatering and physical compaction. Furthermore, calcite cementation now filling the intergranular pore spaces has resulted in gross reduction of porosity (Fig. 10, parts B and C), making it useless as a reservoir rock. The original pores of Petrofacies A, which were mostly foraminiferal chambers and intragranular pores, have all been occluded and packed by calcite cement, which was derived from matrix dissolution along stylolites at the mesogenetic stage. Such stylolites were observed commonly in the Dokan outcrop, and in core samples from the Taq Taq, Kirkuk, and Jambur fields, as well as occasionally in the core intervals from the Bai Hassan and Khabaz fields.

Both cementation and compaction have modified and reduced the connectivity of the pore network by either filling or closing pathways for fluid flow. The permeability of Petrofacies A shows very low permeabilities falling in the range 65 nD–51 μ D (6.41×10^{-20} – 5.03×10^{-17} m²), which indicates a low porosity, a low hydraulic connectivity, or both (Glover and Walker, 2009; Glover, 2010).

We have observed that open fractures, although fairly rare, have an important impact on the enhancement of permeability in some samples by dramatically increasing the hydraulic connectivity of all the petrofacies even if the fractures are rough (Glover et al., 1997). Those 5 samples of Petrofacies A which contain open fractures often have permeabilities over 10 mD (9.87×10^{-15} m²) (i.e., two orders of magnitude greater than the unfractured samples) and are labeled in Fig. 13 as ‘fractured’. It is clear that the fracturing has led to at least a two order of magnitude enhancement of their permeability compared to the rest of the Petrofacies A samples.

However dramatic the effect of open fractures is on the permeability, cemented fractures are much more common in our samples. Cemented fractures, however, have no effect on the overall permeability because the permeability of the matrix is so low already.

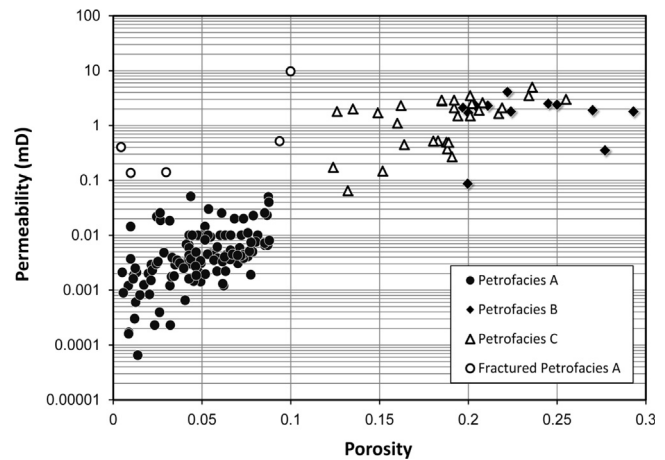


Fig. 13. Porosity–permeability relationships for each of the three main petrofacies, and considering fractured samples of Petrofacies A separately.

4.2.3.2. Petrofacies B. This petrofacies is derived from the wackstone/packstone microfacies. It is the second most dominant petrofacies, which is present patchily in the Bai Hassan and Khabaz fields only. Petrofacies B is characterized by the common occurrence of an enhanced secondary porosity caused by post-depositional dissolution which has given rise to moldic and intergranular pores. The moldic pores are derived from the dissolution of previously filled foraminifera chambers, and can be recognized easily with a polarizing microscope by their bluish trace coloration (Fig. 9, Part C). The median size of the moldic pores in Petrofacies B is much larger than that for Petrofacies A, while the intercrystalline pores, though larger than their Petrofacies A counterparts, remain nanometre in scale. Petrofacies B also shows a marked lack of cementation, as well as a lack of stylolites and vice versa. It is thought that the lack of stylolites meant that a source of dissolved material was unavailable for the cementation of what remained of the primary porosity after compaction, and the lack of cementation subsequently allowed later fluids to further dissolve the matrix in order to arrive at the present day rock fabric.

The XRD samples of this petrofacies showed only small fractions of clay minerals, generally less than 3%. The measured porosity of Petrofacies B is in the range 0.197 ± 0.01 to 0.293 ± 0.01 , i.e., higher than Petrofacies A as a result of the dissolution. The permeability of Petrofacies B is also higher in the range 0.0874–4.1 mD (8.62×10^{-17} – 4.05×10^{-15} m²) than Petrofacies A. This is due to a slightly greater porosity as well as increased pore connectivity.

4.2.3.3. Petrofacies C. The third petrofacies (Petrofacies C) is defined from the mudstone microfacies, where the original fabric of the rock has been dissolved and secondary pores have been formed, improving the reservoir quality. This petrofacies is characterized by a much higher porosity than Petrofacies A, and has similar porosities to Petrofacies B. The common types of pores are intercrystalline pores between calcite crystals and intergranular, which can both be clearly identified in thin-sections (e.g., Fig. 9, Part D).

The size of pores in Petrofacies C is generally greater than for the other two petrofacies, being of micrometer scale, but the percentage of foraminifera grains is smaller than 10%. Both the porosity and the permeability have been enhanced by the dissolution of the ground mass, and macroscopic pores can be seen in hand specimen and filled with blue resin under visible light microscopy (Fig. 10, Parts E and F). The porosity varies in the range 0.124 ± 0.01 and 0.255 ± 0.01 , which makes it a possibly valuable reservoir rock.

The secondary porosity in this petrofacies is commonly caused by syn-diagenetic dissolution. Furthermore, the XRD analysis shows the presence of a small amount of dolomite mineral (7%) which indicates that dolomitization has limited the growth of the secondary porosity. The formation of stylolites and pressure solution in this unit was very rare and only observed locally in the lower part of the Kometan (K2) in the Khabaz field. This is in marked contrast to the extensive effects of stylolites in the Kirkuk, Jambur, and Taq Taq fields, which led to cementation and the destruction of reservoir quality.

The permeability of Petrofacies C is a little lower than the Petrofacies B, in the range 0.065–5.0 mD (6.41×10^{-17} – 4.93×10^{-15} m²) (Fig. 12). This is due to a slightly greater porosity as well as increased pore connectivity (Glover and Walker, 2009; Glover, 2010).

It should be noted that there is a good correlation between the three petrofacies and the three lithological units recognized in the field. The Upper unit (K1) and Lower unit (K2) contain examples of Petrofacies A in the Dokan section, Taq Taq, Kirkuk, and Jambur fields, while it is present in only the Lower unit (K2) in the Bai Hassan and Khabaz fields. Petrofacies B is recorded in the lower part of the Upper unit of the Kometan (K1), and Petrofacies C is observed in the upper part of the Upper unit (K1) of the Kometan in Bai Hassan and Khabaz fields.

4.2.4. Porosity and permeability relationships

Porosity and permeability are perhaps the two most important factors determining reservoir quality. In carbonate reservoirs the porosity and permeability are controlled by the amount and type of porosity and how that porosity is interconnected. These are in turn controlled by diagenetic processes including compaction, dissolution, precipitation and alteration.

Fig. 13 shows the data for all three petrofacies in the form of a poroperm plot. In Petrofacies A, the intercrystalline pores between calcite crystals and original intergranular pores of the foraminifera chambers are totally blocked with calcite cement. The preserved intercrystalline pores do not exceed 0.8 μm (Fig. 10). The matrix permeability is similar to the porosity filled by calcite cement, which limits the enhancement of fluid flow by fractures, leaving only the partially filled calcite fractures and intercrystalline pores as pathways for fluid flow. Consequently, both the porosity and the permeability are extremely restricted, occupying the bottom left-hand side of the poroperm plot. The only exceptions are those 5 samples which contain open fractures. The open fractures do not represent a large increase in the porosity of the sample because they are very localized. However, they increase the hydraulic connectivity and hence the permeability hugely, providing a direct flow path across each sample.

Petrofacies B has undergone post-deformation diagenesis, which has formed its moldic and vuggy porosities. The porosity and permeability of this petrofacies are high but the enhanced permeability is not governed by the porosity improvement. In other words, the dissolution which formed the molds and vugs has not contributed to increasing the connectivity of the pore network, such pores and vugs remaining relatively isolated in the rock matrix.

Petrofacies C has undergone dissolution and possibly dolomitization, creating intercrystalline and intergranular pores, which has augmented the porosity. These processes have not only increased the overall porosity, but have led to an increase in the hydraulic connectivity, especially in the case of the intercrystalline porosity caused by dolomitization. Each augmentation of porosity in this petrofacies is associated with a small increase in the connectivity of the pore network, which also leads to an increase in permeability of the sample as porosity increases.

The poroperm diagram shown in Fig. 13 shows each petrofacies distinctly, with unfractured samples of Petrofacies A well separated in the bottom, left-hand corner due to their low porosity and permeability. Petrofacies A has porosities in the range 0.01–0.08 and a large range of permeabilities, some of which are higher than the permeability of some Petrofacies B and C samples. The large spread of permeabilities reflects the large range of pore connectivity present within this fabric, while the positive trend shows that any small increase in porosity provides an enhancement of the connectivity of the pore network sufficient to increase the permeability of the sample.

The fractured samples of Petrofacies A occupy the top left-hand side of the poroperm diagram because the fractures only raise the porosity by a small amount, but have an extremely large effect on the sample's permeability.

There is some overlap between Petrofacies B and C, but both show significantly larger porosities and correspondingly larger permeabilities. The relatively flat distribution of Petrofacies B shows that increasing porosity (in the range 0.18–0.28) is not significantly enhancing permeability in the sample, which varies from 0.08 mD to 5 mD. This agrees well with our previous observation that newly created molds and vugs tend to be relatively unconnected to the existing pore network. Petrofacies C has a well-constrained porosity range, from about 0.12 to about 0.26, and an equally well-constrained permeability range, from about 0.06 mD to about 4 mD. Overall there is a positive poroperm trend for Petrofacies C showing that higher porosities caused by dissolution also lead to higher permeabilities.

In summary, the cause of the porosities and permeabilities is clear when one compares the poroperm plot with the photomicrographs of each petrofacies. Petrofacies A has low porosities and it is relatively unconnected thanks to a well-developed calcite-rich cementation. Petrofacies C has a rock fabric that has undergone substantial dissolution and dolomitization leading to significant secondary porosity, and consequently higher permeabilities. Petrofacies B, however, while also dissolved, has undergone post-depositional dissolution leading to significant secondary porosity, but including relatively isolated molds and vugs. Petrofacies B and C are very common in the south of the Kirkuk embayment with an intercalation with three different rock units (Sa'di, Tanuma and Khasib), and are characterized in the field by clearly visible macroporosity, each representing a high-quality potential reservoir rock.

4.2.5. Permeability modeling

Although it was not the object of this paper to model the poroperm relationships for the petrofacies of the Kometan Formation, we have carried out a simple power law fit to all of the data which showed no fracturing. This procedure gives the permeability k (mD) = $28.044\phi^{2.6504}$ with $R^2=0.703$, as shown in Fig. 14.

We have also applied the RGPZ model (Glover et al., 2006), which is derived from the theory of the electrical properties of saturated rocks (Glover et al., 1994; Revil and Glover, 1997, 1998). The RGPZ model is not empirical, taking the form

$$k_{\text{RGPZ}} = \frac{d^2 \phi^{3m}}{4am^2} \quad (1)$$

where d is the modal grain diameter (in m), ϕ is the porosity (fractional), m is the cementation exponent (dimensionless) and a is a constant that is thought to be close to $8/3$ for porous granular media, but may be different for tight carbonates. We found that a cementation exponent $m=1.5$ and a modal grain diameter $d=10^{-5}$ m fitted the aggregated data best ($R^2=0.82$). The fitted cementation exponent is close to what would be expected for a random packing of pluridisperse spheres ($m=1.5$) and differs from

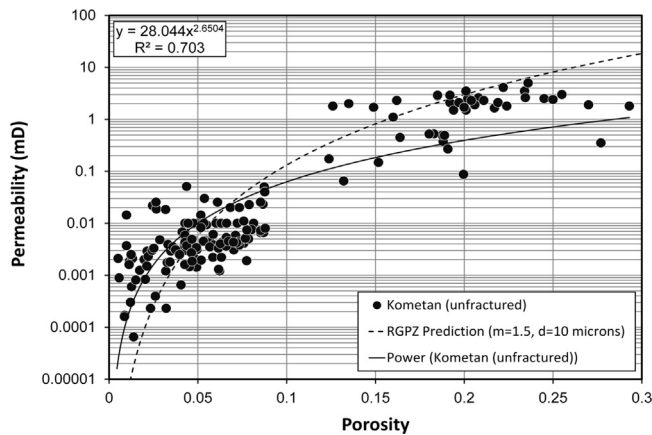


Fig. 14. Permeability modeling taking all the samples as a single dataset. Solid line: power law fit with k (mD) = $28.044\phi^{2.6504}$ with $R^2 = 0.703$. Dashed line: RGPZ model (Glover et al., 2006) $m = 1.5$ and $d = 10 \mu\text{m}$ ($R^2 = 0.82$). Better fits are available if one considers each petrofacies separately.

values typical of sandstones ($1.7 < m < 2.1$) or for well-cemented carbonates ($2 < m < 4$), and probably arises from the relatively granular/crystalline nature of the microstructure as seen in Fig. 10. The modeled grain diameter is in good general agreement with the overall grain diameter, as imaged using the high resolution SEM (Fig. 10). However, in both cases, we would expect a better fitting with more accurate and specific parameters to arise from fittings of the RGPZ model to individual petrofacies, while the RGPZ model should benefit from the implementation of values of d and m specific to each rock sample, both of which will be the subject of a further paper.

4.2.6. Petrofacies distinction from well logs

The question arises whether it is possible to distinguish between three important petrofacies using wireline tool data. It is clear from Figs. 11 and 13 that isolating Petrofacies A is relatively simple. It can be done on the basis of porosity alone, and is defined as that rock within the Kometan Formation which has a porosity less than 10%, i.e., $\phi < 0.1$. Distinguishing between the petrofacies of reservoir quality that remain, i.e. Petrofacies B and Petrofacies C, is more difficult and cannot be done using porosity or permeability. However, we have noticed that a distinction can be made on the basis of NMR T_2 relaxation time spectra (Fig. 15).

The interpretation of the NMR T_2 spectra for the tight Kometan carbonates differs significantly from that for normal clastic rocks in several ways. To begin, all the usual T_2 cut-off values will not be valid. Second, the clay content of all of the petrofacies is extremely small (< 3% by volume), and hence peaks associated with clay-bound water are extremely small or non-existent, and may be subsumed within the tails of other larger peaks. Third, the extremely large variation in pore size between all of the petrofacies is the main controlling factor on where peaks occur on the T_2 spectrum.

The NMR T_2 relaxation time spectrum for Petrofacies A shows a small peak between 0.1 ms and 5 ms, which is associated with the capillary-bound water existing in nanometric scale pores. A second, larger peak between 5 ms and 50 ms is associated with mobile water in these extremely small pores. The T_2 cut-off between the capillary-bound water and the mobile water occurs at about 2.66 ms. Whatever T_2 behavior that might be associated with small amounts of clay-bound water is indistinguishable from the capillary-bound peak.

Petrofacies C has a very similar style, but peaks occur at larger values of T_2 . Once again there is a small peak for capillary-bound

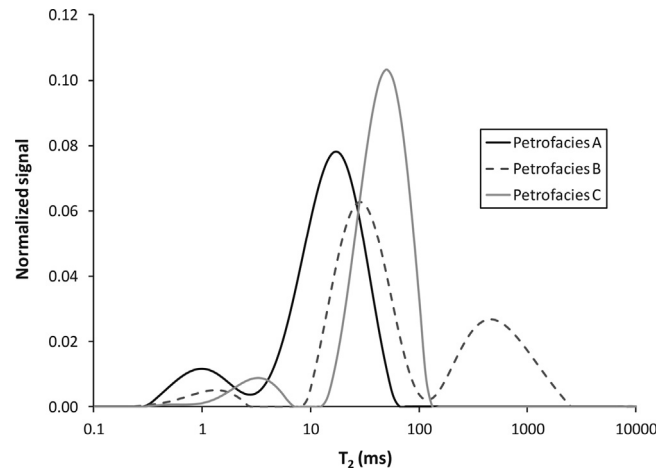


Fig. 15. Typical NMR T_2 spectra for each of the petrofacies defined in this work.

water, but this occurs in the range 1–6 ms. The higher values of T_2 are associated with capillary bound water occurring in the larger-sized pores in Petrofacies C; about 10–100 times larger than their equivalents in Petrofacies A. There is a second, much larger peak which occurs between 10 ms and 100 ms, and which is associated with mobile fluids in the larger pores of this petrofacies. Consequently, Petrofacies C is similar to Petrofacies A except both the capillary bound and mobile fluid peaks occur at higher T_2 values in Petrofacies C because it contains much larger pores; pores of a size similar to those which might occur in a clastic rock. Consequently, the cut-off between the capillary-bound water and the mobile fluids in Petrofacies C, which occurs at 10 ms, is closer to the 33 ms value often used as a rule-of-thumb for clastic rocks. Once again, whatever T_2 behavior that might be associated with small amounts of clay-bound water in Petrofacies C is indistinguishable from the capillary-bound peak.

The NMR T_2 relaxation time spectrum for Petrofacies B is significantly different. While it shares the small peak at small T_2 relaxation times (between 0.1 ms and 5 ms) that represents capillary-bound water, we found that the mobile water splits into two clearly distinguishable peaks. The first one occurs between 10 ms and 100 ms and represents the mobile fluid in the inter-crystalline pores of the rock. A second, moderately sized peak occurs between 100 ms and 2000 ms, and this is associated with mobile fluids occupying the very large moldic and vuggy porosity in this petrofacies. The T_2 cut-off between the capillary-bound water and the intercrystalline mobile water occurs at about 5 ms, while the T_2 cut-off between the two types of mobile fluid occurs at approximately 100 ms.

Distinction between Petrofacies A and C on the basis of NMR T_2 spectra is not on the basis of different spectra patterns, but on the positions of the peaks which are controlled by the size of the pores in each petrofacies. Whereas distinction between Petrofacies B and the other two is simple because Petrofacies B has two mobile fluid peaks, one for intercrystalline flow and one for flow controlled by the moldic porosity.

5. Conclusions

The main conclusions of this research are summarized as follows:

1. Stratigraphic and sedimentological studies of the outcrop section and available samples have shown that the Kometan Formation can be divided into two lithological units: (i) a globigerinal limestone, Upper unit (K1), and (ii) a mixed

oligosteginal and globigerinal limestone unit, Lower unit (K2). A shaly limestone unit (Ksh) intercalates between these two units toward the western margin of the Kirkuk embayment.

2. A petrophysical, petrographic and visual study identified three types of petrofacies: (i) Petrofacies A, which is characterized by dense and compacted and cemented wackstone/packstone that includes nanometer size intercrystalline pores and contains significant stylolites, (ii) Petrofacies B, which is a dissolved wackstone/packstone that contains moldic and vuggy pores, and (iii) Petrofacies C, identified as a carbonate mudstone that has undergone dissolution and possibly some dolomitization.
3. The porosity and permeability of the compacted wackstone/packstone petrofacies (Petrofacies A) were very low, indicating a poor reservoir quality, while the other two petrofacies (Petrofacies B and C) had higher porosities and permeabilities and can be considered as good reservoir quality.
4. The presence and distribution of open fractures has an impact on reservoir quality. The presence of fractures can act as both a barrier to fluid flow or enhance reservoir quality depending on whether the fractures are open or closed within all three different petrofacies. Open fractures occurring in Petrofacies A often result in a 2–3 order of magnitude increase in permeability with little enhancement of overall porosity.
5. The pore systems in the various petrofacies of the Kometan Formation are governed strongly by diagenetic process and tectonic fractures, which enhance pore network connectivity and reservoir permeability.
6. Cementation and consequent porosity and permeability reduction in Petrofacies A is associated with significant formation of stylolites, and it has been suggested that the process of stylolite formation is the source of the cementing material.
7. All three petrofacies can be distinguished from wireline log data. The use of porosity alone is sufficient to isolate Petrofacies A, where this petrofacies has values porosity, $\phi < 0.1$. Neither porosity nor permeability is capable of distinguishing between Petrofacies B and Petrofacies C. However, NMR measurements show that Petrofacies B has a well-developed additional peak in its T_2 relaxation spectrum occurring above 100 ms and associated with large moldic and vuggy pores.

Acknowledgments

This study was funded by the Ministry of Higher Education of the Iraqi Kurdistan Region government as a part of the Human Capacity Development Programme (HCDP) that is greatly appreciated. We express our gratitude to the Ministry of Natural Resources of Kurdistan Region and the Ministry of Oil of the Iraqi government for providing the project data.

References

Abawi, T.S., Mahmood, S.A., 2005. Biostratigraphy of the Kometan and Gulneri Formations (Upper Cretaceous) in Jambur well No. 46, Northern Iraq. *Iraqi J. Earth Sci.* 5 (1), 1–8.

Al-Qayim, B., 2010. Sequence stratigraphy and reservoir characteristics of the Turonian–Coniacian Khasib Formation in Central Iraq. *J. Pet. Geol.* 33 (4), 387–404 2010.

Al-Sakini, J.A., 1992. Summary of Petroleum Geology of Iraq and the Middle East. Northern Oil Company Press, Kirkuk (in Arabic).

Aqrabi, A.A.M., Horbury, A.D., Goff, J.C., Sadooni, F.N., 2010. The Petroleum Geology of Iraq. Scientific Press Ltd, Beaconsfield, UK 424 pp.

Aqrabi, A.A.M., 1996. Carbonat–siliciclastic sediments of the Upper Cretaceous (Khasib, Tanuma and Sa'di Formations) of the Mesopotamian Basin. *J. Mar. Pet. Geol.* 13 (7), 781–790.

Buday, T., 1980. The Regional Geology of Iraq. V.L.; Stratigraphy and Paleogeography. S.O.M. Library, Baghdad 350 pp.

Choquette, P.W., Pray, L.C., 1970. Geological nomenclature and classification of porosity in sedimentary carbonates. *AAPG Bull.* 54 (2), 207–250.

Dunham, R.J., 1962. Classification of carbonate rocks according to depositional texture. In: Ham, W.E. (Ed.), *Classification of Carbonate rocks*, vol. 1. AAPG-Publication, Tulsa, Oklahoma, pp. 108–121.

Dunnington, H.V., 1958. Generation, migration, accumulation, and dissipation of oil in northern Iraq, in *Habitat of oil*: AAPG Spec. Publ., 1194–1251.

Feazel, C.T., Schatzinger, R.A., 1985. Prevention of carbonate cementation in petroleum reservoirs. In: Schneidermann, N., Harris, P.M. (Eds.), *Carbonate Cements*, vol. 36. SEPM Special Publ., pp. 97–106.

Garland, C.R., Abalioglu, I., Ackca, L., 2010. Appraisal and development of the Taq Taq field, Kurdistan region, Iraq. In: *Proceedings of the Petroleum Geology Conference Series*, pp. 801–810.

Glover, P.W.J., 2010. A generalized Archie's law for n phases. *Geophysics* 75 (6), E247–E265. <http://dx.doi.org/10.1190/1.3509781>.

Glover, P.W.J., Walker, E., 2009. Grain-size to effective pore-size transformation derived from electro-kinetic theory. *Geophysics* 74 (1), E17–E29. <http://dx.doi.org/10.1190/1.3033217>.

Glover, P.W.J., Zadjali, I.I., Frew, K.A., 2006. Permeability prediction from MICP and NMR data using an electrokinetic approach. *Geophysics* 71 (4), F49–F60.

Glover, P.W.J., Matsuki, K., Hikima, R., Hayashi, K., 1997. Fluid flow in fractally rough synthetic fractures. *Geophys. Res. Lett.* 24 (4), 1803–1806. <http://dx.doi.org/10.1029/97GL01670>.

Glover, P.W.J., Meredith, P.G., Sammonds, P.R., Murrell, S.A.F., 1994. Ionic surface electrical conductivity in sandstone. *J. Geophys. Res.* 99 (B11), 21635–21650.

Halley, R.B., Schmoker, J.W., 1983. High porosity Cenozoic carbonate rocks of South Florida: progressive loss of porosity with depth. *AAPG Bull.* 67, 191–200.

Iranpanah, A., Efsandiari, B., 1979. Structural evolution and correlation of tectonic events in the Alborz Mountains, the Zagros Range and Central Iran. *Bulletin. Soc. Belg. Géol.* 88, 285–295.

Jassim, Z.J., Goff, J.C., 2006. The Geology of Iraq. Dolin, Prague.

Jones, S.C., 1997. A technique for faster pulse-decay permeability measurements in tight rocks. In: *Proceedings of the SPE* 28450.

Karim, K.H., Taha, Z.A., 2009. Tectonical history of Arabian platform during Late Cretaceous: an example from Kurdistan region, NE Iraq. *Iran. J. Earth Sci.* 1, 1–14.

Kaddouri, N., 1982. Tel Hajar: A new Cenomanian–Lower Turonian Stratigraphic Unit from North-west Iraq. *Cretaceous Research*. Academic Press Inc., London, pp. 391–395.

Mazzullo, S.J., Chilingarian, G.V., 1992. Diagenesis and origin of porosity. In: Chilingarian, G.V., Mazzullo, S.J., Rieke, H.H. (Eds.), *Carbonate Reservoir Characterization: A Geologic-Engineering Analysis*, Part I, vol. 30. Elsevier Publ. Co., Amsterdam, Developments in Petroleum Science, pp. 199–270.

Ramsay, J.G., Huber, M.I., 1983. The Techniques of Modern Structural Geology, 1: Strain Analysis. Academic Press, London 307 pp.

Revil, A., Glover, P.W.J., 1997. Theory of ionic surface electrical conduction in porous media. *Phys. Rev. B* 55 (3), 1757–1773.

Revil, A., Glover, P.W.J., 1998. Nature of surface electrical conductivity in natural sands, sandstones, and clays. *Geophys. Res. Lett.* 25 (5), 691–694.

Rowland, S.M., Duebendorfer, E.M., Schiefelbein, I.M., 2007. Structural Analysis and Synthesis: A Laboratory Course in Structural Geology, third edition Blackwell Publishing Ltd. 301 pp.

Sadooni, F.N., 2004. Stratigraphy, depositional setting and reservoir characteristics of Turonian–Campanian carbonates in Central Iraq. *J. Pet. Geol.* 27 (4), 357–371.

Sattarzadeh, Y., Cosgrove, J.W., Vita-Finzi, C., 2000. The interplay of faulting and folding during the evolution of the Zagros deformation belt. In: Cosgrove, J.W., Ameen, M.S. (Eds.), *Forced Folds and Fractures*, vol. 169. Geol. Soc., London, Spec. Publ., pp. 187–196.

Taq Taq Operation Company (TTOPCO), 2007. Geological Report.

Wardlaw, N.C., 1996. Factors affecting oil recovery from carbonate reservoirs and prediction of recovery. In: Chilingarian, G.V., Mazzullo, S.J., Rieke, H.H. (Eds.), *Carbonate Reservoir Characterization: A Geologic-Engineering Analysis*, Part II, vol. 44. Elsevier Publ. Co., Amsterdam, Developments in Petroleum Science, pp. 867–903.

van Bellen, R.C., Dunnington, H.V.G., Wetzel, R., Morton, D.M., 1959. *Lexique Stratigraphique international*, III, Asie, fasc. 10a, Iraq. Centre national de la recherche scientifique, Paris p. 333.

Vernant, P.H., Nilforoushan, F., Hatzfeld, D., Abbassi, M.R., Vigny, C., Masson, F., Nankali, H., Martinod, J., Ashtiani, A., Bayer, R., Tavakoli, F., Chery, J., 2004. Present-day crustal deformation and plate kinematics in the Middle East constrained by GPS measurements in Iran and northern Oman. *Geophys. J. Int.* 157, 381–398.